Effect of Prestatic Loading on Dynamic Tensile Strength of Concrete under High Strain Rates

Xudong Chen, Ph.D., A.M.ASCE[1]; Limei Ge[2]; Haotian Yuan[3]; and Jikai Zhou[4]

Abstract: The static bending tests and the split Hopkinson pressure bar (SHPB) dynamic bending tests of concrete are investigated in this paper, and the effects of different initial static loading history on the dynamic tensile strength of concrete are explored. The initial static loadings are divided into five grades, 0, 25, 50, 75, and 90% of static tensile strength, respectively. A large number of mesostructure images of specimens have been obtained by the means of a scanning electron microscope (SEM) and used to analyze the influence of the microstructure and microcrack propagation on the dynamic performance of concrete. In addition, the Weibull distribution model is introduced to analyze the test results, which show that the dynamic tensile strength of concrete increases significantly with an increase in strain rate. When the initial static loading level does not exceed 50%, dynamic tensile strength is basically stable; but when the initial static loading level is more than 75%, dynamic strength begins to decrease. **DOI: 10.1061/(ASCE)MT.1943-5533.0001698.**

Author keywords: Prestatic loading; Statistical model; Dynamic tensile strength; Concrete.

Introduction

Extreme loads, such as impacts and blasts, occur at high strain rates of loading, generating a large amount of energy (Gupta and Seaman 1978; Cunliffe et al. 2015). Therefore, when evaluating the mechanical properties of a structure and its constituent materials, the influence of loading history has to be taken into consideration. However, the initial loading history includes various types, such as static tensile loading, compression loading, cyclic loading, and fatigue loading, all of which affect the mechanical properties of the structure or materials to a certain extent. Therefore, a variety of damage phenomena caused by the initial loading history has great effect on the structure and properties of concrete engineering, which has important research significance.

In recent years, many domestic and foreign scholars have studied the dynamic mechanical properties of concrete (Chen et al. 2013, 2014a) materials under initial static loading, and some researchers analyzed concrete microstructure changes under different loading conditions with the help of scanning electron microscopes (Derucher 1978; Uchikawa et al. 1997; Konin et al. 1998; Bisschop and Van Mier 2002; Wang et al. 2005). Tinic and Brühwiler (1985) investigated the effect of compressive loads on the tensile strength of concrete at a high strain rate. They considered that the tensile strength decreased remarkably due to the compression-damage effect. Cornelissen and Reinhardt (1984) studied the influence of the static and fatigue preloading on the residual strength of plain concrete. They considered that the static tensile preloading had little influence on the tensile or compressive strength of the concrete, but compressive strength was not affected by the static compressive preloading. Gettu et al. (1996) researched the influence of monotonic and cyclic compression loading history on the splitting tensile strength of high-strength concrete. They concluded that the compression damaging could lead to a significant decrease in tensile strength. Lin et al. (2002) and Lu et al. (2004) explored the reduction of tensile strength and compressive strength of concrete due to triaxial compressive loading history, respectively. Soroushian and Elzafraney (2004) studied several damage effects on concrete performance and microstructure. These damaging effects include compression, impact, fatigue, and freeze-thaw cycles. In addition, trends in microcrack growth under such damaging effects on concrete properties were justified based on results gained using scanning electron microscopes (SEM). Lin et al. (2007) studied the dynamic tensile properties of concrete under initial static loading and concluded that the higher the initial static loading, the lower the dynamic tensile strength of concrete. Yan and Lin (2008) researched the influence of initial static stress on the dynamic mechanical properties of concrete and believed that the ultimate dynamic strength of concrete decreased gradually with an increase of initial static stress. Xiao et al. (2010, 2011) studied the influence of strain rates and loading histories on tensile and compressive damage behavior of concrete. Wu et al. (2014) studied the effect of predamage on the stress-strain relationship of FRP concrete under monotonic loading. Singh et al. (2015) carried out an experimental study on uniaxial compressive strength (UCS) of rock under preloading with tensile stress and improved the traditional Brazilian disc test. They considered that if preloading tensile stress exceeded about half of the Brazilian tensile strength, stress removal had a substantial effect on the UCS, and conservative results may be expected from laboratory tests on rock specimens.

To summarize, some scholars considered that initial static loading could increase or decrease the dynamic strength (Tinic and Brühwiler 1985; Gettu et al. 1996; Lin et al. 2007; Yan and Lin 2008; Singh et al. 2015); others thought that the initial static

[1]Lecturer, College of Civil and Transportation Engineering, Hohai Univ., Nanjing, Jiangsu 210098, P.R. China (corresponding author). E-mail: cxdong1985@hotmail.com

[2]Graduate Student, College of Civil and Transportation Engineering, Hohai Univ., Nanjing, Jiangsu 210098, P.R. China. E-mail: glm2802@163.com

[3]Graduate Student, College of Civil and Transportation Engineering, Hohai Univ., Nanjing, Jiangsu 210098, P.R. China. E-mail: 18351967156@163.com

[4]Professor, College of Civil and Transportation Engineering, Hohai Univ., Nanjing, Jiangsu 210098, P.R. China. E-mail: zhoujikaihhu@163.com

Note. This manuscript was submitted on January 8, 2016; approved on May 25, 2016; published online on July 20, 2016. Discussion period open until December 20, 2016; separate discussions must be submitted for individual papers. This technical note is part of the ***Journal of Materials in Civil Engineering***, © ASCE, ISSN 0899-1561.

loading had little or no influence on the dynamic strength of concrete (Cornelissen and Reinhardt 1984).

In this paper, the dynamic tensile properties of concrete under different initial static loadings are explored by the static bending tests and split Hopkinson pressure bar (SHPB) dynamic bending tests (Chen et al. 2014b). The initial static loadings are divided into five grades: 0, 25, 50, 75, and 90% of static bending strength, respectively. A scanning electron microscope (SEM) is chosen to obtain a large number of mesostructure images of specimens and analyze the influence of microcrack propagation on the dynamic performance of concrete. At the same time, the Weibull distribution model is introduced to analyze the test results, and the damage mechanism of the dynamic tensile strength of concrete under the initial static loading is further discussed later.

Experimental Program

Test Procedure

The experimental study is completed according to the following four steps:

1. Determine the static tensile strength of concrete σ_{st};
2. Divide the specimens into five groups; each group contains 30 members and applies the initial tensile stress respectively, as determined in the first step. The five grades are 0, 25, 50, 75, and 90% of the static tensile strength σ_{st};
3. Determine the dynamic tensile strength of concrete σ_{dt} under different initial static load conditions with three different strain rates; and
4. Five specimens selected from the five groups from Step 2 were the subject of electron microscope scanning tests, respectively.

In this procedure, a 10 kN universal testing machine for the static tensile test (three-point bending) is applied in the first and second steps. The SHPB device is used for the dynamic tensile test of concrete in the third step, and the effect of strain rate is considered.

Materials Preparation

In this paper, rectangular concrete specimens with the size of 40 × 40 × 160 mm were used. The cementitious materials for concrete are ordinary portland cement of Grade 42.5 and Grade I fly ash according to Chinese standard [GB/T-50146 (GB/T 2014)]. The water to cement ratio for concrete is 0.38. Fine aggregates are river sands, which are mainly composed of quartz, and contain 10% of feldspar. Coarse aggregates are crushed stones having a maximum particle size of 10 mm. The particle size range of sand is 0.4–2.5 mm continuous gradation. In order to increase the liquidity of the mixture, 1% mass fraction of polycarboxylate superplasticizer was added and mixed. The mix proportions are listed in Table 1.

The templates were cleaned, assembled, and brushed with machine oil before the tests. In the process of casting, the cement, fly ash, sand, and gravel were firstly mixed and stirred for 1 min. Then the weighed water reducer and the water was fully mixed with aggregate and stirred for 3 min. Finally, the mixed concrete was poured in the prepared steel mold and placed on a low speed vibration table for vibration compacting. The surface of the specimen was smoothed 1 h after casting. The specimens then were covered and cured for 24 h before form removal. At last, the specimens were placed into a saturated solution of calcium hydroxide curing for 28 days in room-temperature conditions. A month later, the specimens were taken out and placed in the laboratory for natural curing.

Table 1. Mix Proportion for Concrete

Concrete compositions (kg/m^3)						Water to cementitous ratio
Water	Cement	Sand	Coarse aggregate	Fly ash	Water reducer	
180	380	668	1,089	94	4.75	0.38

Static Tensile Tests

The static bending test of concrete is an applied load according to ASTM C293-02 (ASTM 1979). The specimen is damaged along the center position in general where the bending moment is maximum. In order to measure the tensile stress of the section, calculations are carried out according to the following formula:

$$\sigma_{st} = \frac{3FL}{2bh^2} \tag{1}$$

where σ_{st} = static tensile strength; F = maximum load at failure, b and h = width and height of the specimen, respectively; and $L = 120$ mm = distance between supports.

The specific test procedure is as follows. Firstly, the 10–15 specimen are taken out to carry out static bending test, and then the static tensile strength of concrete is determined by Weibull distribution model. Then, the 150 specimens are divided into five groups and numbered as 0, 1, 2, 3, and 4 (for example, the number of second group is 1-1, 1-2 etc., through to 1-30). Finally, the static test is carried out using the universal testing machine. The initial static loading is applied following five grades: 0, 25, 50, 75, and 90%) × σ_{st}.

Dynamic Tensile Tests

The dynamic bending tests using the five groups of specimens that have been subject to the initial static loadings are carried out using a SHPB device, as shown in Fig. 1. Concrete specimens are fixed between the incident and transmission bars with a three-point bending heel block, which could ensure the specimens remain in the bending state, as shown in Fig. 2. By adjusting the air pressure, the projectile obtained various velocities to impact the incident bar and generated the stress wave. When the waves spread to the interface between the specimen and incident bar, due to their material impedance mismatch, the stress waves reflected on the interface. The incident wave $\varepsilon_i(t)$ and the reflected wave $\varepsilon_r(t)$ are recorded by two strain gauges pasted in the middle of the incident bar. The main parameters are given in Tables 2 and 3.

The impact velocity V_c and impact force F_c between the incident bar and the specimen could be calculated using the classical kinetic equation and momentum conservation:

$$V_c(t) = -C_B[\varepsilon_i(t) - \varepsilon_r(t)] \tag{2}$$

$$F_c(t) = -C_B Z_B[\varepsilon_i(t) + \varepsilon_r(t)] \tag{3}$$

where $C_B = \sqrt{E_B/\rho_B}$ wave velocity in the bars; and $Z_B = E_B A_B/C_B$ = material impedance of the pressure bars.

Delvare et al. (2010) proposed a model that was suitable for quasi-brittle materials, namely the long-beam model. The model takes into account the following two assumptions:

1. The simplified beam is only affected by the bending moment and the torque produced by the shearing force is neglected; and
2. The cross section of the specimen is maintained as a plane and is perpendicular to the axis of the beam.

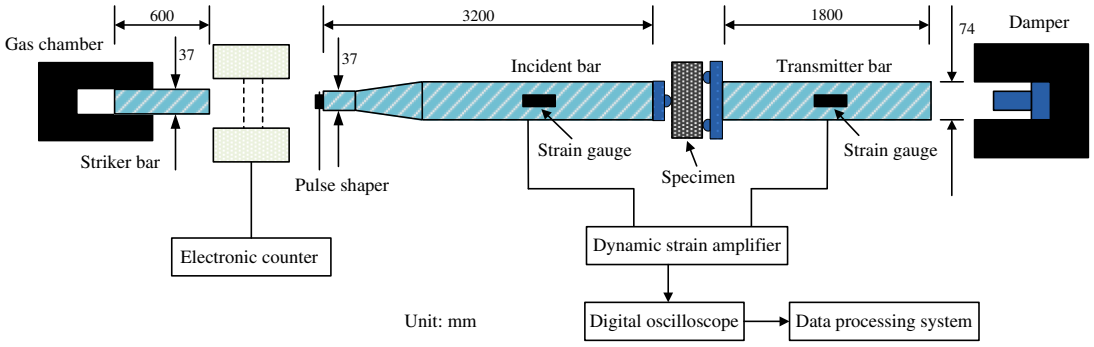

Fig. 1. SHPB dynamic bending system

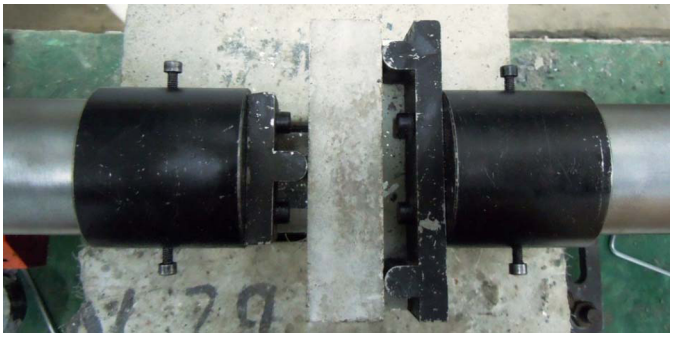

Fig. 2. Loading device of dynamic three-point bending test

Table 2. Pressure Bar Dimensions

Dimension	Size
Length of striker	$L_I = 600$ mm
Length of incident bar	$L_B = 3200$ mm
Diameter of pressure bars	$\phi_B = 74$ mm
Sectional area of pressure bars	$A_B = 4.3 \times 10^{-3}$ m^2

Table 3. Physical Properties and Parameters for Pressure Bars

Physical property	Value
Density	$\rho_B = 7850$ kg/m^3
Elasticity modulus	$E_B = 210$ GPa
Velocity of elastic wave	$C_B = 5172$ m/s
Wave impedance	$Z_B = 174587$ kg/s

The long-beam model has been used in compression tests (Zhao and Gary 1996), which are also applicable to data analysis of the bending tests. In order to accurately describe the experimental elastic response process, the incident and reflected waves need to keep pace. Therefore, it is necessary to modify the reflected wave obtained from the tests, and then calculate the impact velocity and impact force of the specimens. Due to the fact that the dynamic tensile strength is proportional to the velocity of impact point, the strain rate is proportional to the acceleration of impact point, so dynamic tensile strength and strain rate of specimens can be obtained.

In addition, considering the effect of strain rate $\dot{\varepsilon}$ on the dynamic tensile strength of concrete, each group of 30 specimens is divided into three groups of 10. Dynamic impact tests are carried out at three air pressure levels of 0.10, 0.15, and 0.20 MPa. Each impact waveform is recorded and the results will be discussed later.

Weibull Distribution Model

Because of the high dispersion of brittle materials such as concrete and in order to describe the static and dynamic characteristics of concrete more accurately, the Weibull distribution model is introduced to analyze the reliability and dispersion. The standard Weibull equation is

$$P = 1 - e^{-\left(\frac{\sigma-\sigma_u}{\sigma_0}\right)^m} \tag{4}$$

where P = failure probability; σ = variable parameter; σ_u = minimum critical stress whose failure probability is close to zero; m = Weibull modulus, also called the shape parameter; and σ_0 = scale parameter.

The critical value σ_u is difficult to be determined according to the test, because it appears at the end of the model with low strength, and it almost has no impacts on the results. In order to achieve linear fitting, both sides of Eq. (4) are taken by the double logarithm as follows:

$$\ln\left[\ln\left(\frac{1}{1-p}\right)\right] = m\ln(\sigma) - m\ln(\sigma_0) \tag{5}$$

The relationship between $\ln(\sigma)$ and $\ln[\ln(1/1-p)]$ could be expressed as a linear equation. Calculation of the value of P is generally based on the probability index function. The common form of probability index is $P = i/(n+1)$ where n is the number of data points and i is the serial number of a point. For any set of test data, the data would first be arranged in ascending order and numbered as $1, 2, 3, \ldots, i$. Then the value of P was calculated, and the curve between $\ln(\sigma)$ and $\ln[\ln(1/1-p)]$ could be drawn. Finally, the linear regression method is used to determine the value of m and σ_0.

Figs. 3(a and b) are the fitting curves and probability distributions of static tensile strength, which are obtained by using the Weibull distribution. The fitting parameter m is 11.80, σ_0 is 11.965, and the correlation coefficient $R^2 = 0.970$. The strength value corresponding to a failure probability of 50% is used as the tensile strength, that is, σ_{st} is 11.60 MPa.

Results and Discussion

Dynamic Tensile Strength

The typical dynamic bending fracture mode of concrete is shown in Fig. 4. The dynamic tensile strength of initial static loading under different strain rates is given in Table 4. It can be seen that with the increase in strain rates, the dynamic tensile strength of concrete clearly increased.

Each group of test data was calculated using the Weibull distribution model. This approach was the same one used previously to

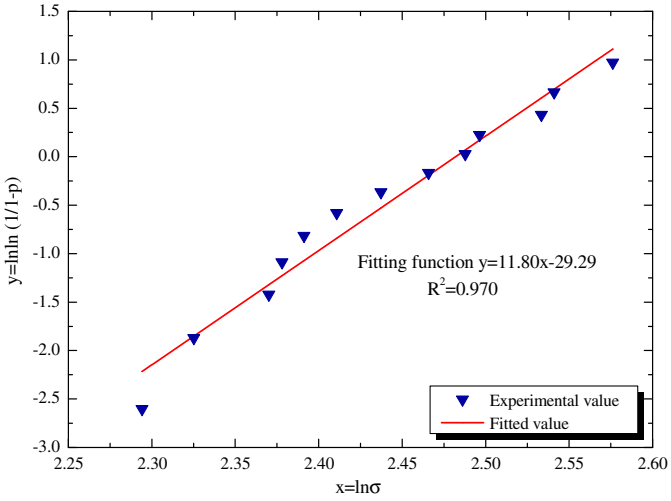

Fig. 3. Quasi-static test curves obtained by Weibull distribution: (a) fitting curve; (b) probability distribution

Fig. 4. Typical fracture pattern of concrete specimen

determine the static tensile strength; a 50% probability is taken as the dynamic tensile strength of concrete. The influence of initial static loading on dynamic tensile strength of the concrete under different strain rates is shown in Fig. 5. It can be seen that concrete's dynamic tensile strength increased significantly as strain rates increased. The effect of initial static loading was also quite obvious under the same strain rate. Changes in dynamic strength mainly depended on the magnitude of the initial static loading in such conditions. When applied in static loading that did not exceed 50% of the peak static strength, the specimens were in the elastic stage at this time, and the dynamic strength of concrete remained basically unchanged. However, when the initial static loading level was more than 75%, the specimens entered into plastic stage and the dynamic strength decreased gradually with increases in initial static loading.

Table 4. Dynamic Tensile Strength of Concrete after Initial Static Loading (Unit: MPa)

	Strain rate of 14.56/s		Strain rate of 26.45/s		Strain rate of 40.58/s	
Initial static loading	Specimen number	Dynamic bending strength	Specimen number	Dynamic bending strength	Specimen number	Dynamic bending strength
0% (0 MPa)	0-1	22.35	0-11	41.87	0-21	59.17
	0-2	30.09	0-12	36.49	0-22	54.43
	0-3	32.40	0-13	35.76	0-23	59.94
	0-4	23.99	0-14	38.94	0-24	56.07
	0-5	25.25	0-15	33.72	0-25	54.02
	0-6	19.18	0-16	34.17	0-26	56.32
	0-7	31.42	0-17	40.46	0-27	54.08
	0-8	28.42	0-18	41.21	0-28	51.30
	0-9	27.30	0-19	39.15	0-29	56.22
	—	—	—	—	0-30	48.00
25% (2.89 MPa)	1-1	23.43	1-11	42.30	1-21	50.83
	1-2	21.13	1-12	42.32	1-22	58.47
	1-3	28.22	1-13	34.53	1-23	58.35
	1-4	30.54	1-14	36.49	1-24	57.86
	1-5	29.38	1-15	36.32	1-25	53.12
	1-6	25.74	1-16	34.83	1-26	55.64
	1-7	21.69	1-17	34.03	1-27	56.84
	1-8	22.41	1-18	39.16	1-28	54.95
	1-9	29.47	1-19	37.50	1-29	55.39
	—	—	1-20	45.59	1-30	53.53
50% (5.79 MPa)	2-1	27.22	2-11	38.14	2-21	56.67
	2-2	21.77	2-12	37.90	2-22	53.89
	2-3	26.61	2-13	34.24	2-23	52.28
	2-4	24.16	2-14	40.52	2-24	55.82
	2-5	26.57	2-15	36.89	2-25	54.63
	2-6	26.90	2-16	36.40	2-26	53.02
	2-7	25.16	2-17	37.11	2-27	55.02
	2-8	27.39	2-18	34.99	2-28	57.65
	2-9	30.77	2-19	40.52	2-29	55.75
	2-10	26.85	2-20	40.58	2-30	53.02
75% (8.69 MPa)	3-1	27.10	3-11	30.83	3-21	52.63
	3-2	23.15	3-12	29.66	3-22	53.55
	3-3	27.89	3-13	36.04	3-23	54.12
	3-4	21.76	3-14	45.88	3-24	51.19
	3-5	23.40	3-15	37.03	3-25	53.71
	3-6	22.82	3-15	46.87	3-26	52.04
	3-7	22.63	3-17	39.24	3-27	56.04
	3-8	27.83	3-18	32.12	3-28	52.13
	—	—	3-19	28.92	3-29	50.28
	—	—	3-20	30.04	3-30	51.63
90% (10.43 MPa)	4-1	17.79	4-11	27.92	4-21	50.35
	4-2	18.88	4-12	28.55	4-22	52.11
	4-3	22.55	4-13	33.38	4-23	48.70
	4-4	21.53	4-14	34.12	4-24	49.50
	4-5	17.64	4-15	28.75	4-25	48.57
	4-6	22.03	4-16	29.14	4-26	52.89
	4-7	20.53	4-17	28.81	4-27	52.97
	4-8	22.79	4-18	28.80	4-28	49.08
	4-9	17.15	4-19	27.70	4-29	48.09
	—	—	4-20	30.48	—	—

Microstructural Investigation

Specimens from the five groups were prepared for the scanning electron microscope (SEM) tests. The SEM machine is a Hitachi

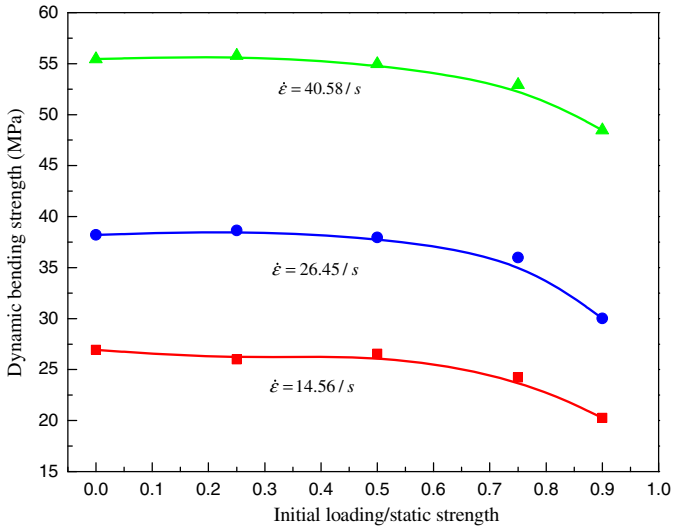

Fig. 5. Influence of initial loading on the dynamic tensile strength of concrete under different strain rates

(Japan) S-4800 type, and the accelerating voltage is 20.0 kV. A large number of microscopic structure pictures were gained under the five different static loadings by means of SEM. The microstructural photos under different initial static loadings were all at 150× or 500× magnification, as shown in Fig. 6.

Fig. 6(a) shows the distribution of microcracks in concrete prior to any damaging effects. Due drying and self-shrinkage interaction, some fine cracks would be present in concrete and aggregate–paste interfaces or joints even if no static loading was applied. However, most of the fine cracks were effectively prevented from extending and connecting to each other by the aggregate.

Until 50% static loading level was applied to the specimen, the fine cracks around the aggregate extended slowly and the width of microcracks gradually deepened. The adjacent cracks connected mutually and the microcrack propagation path was rather tortuous without any rules, which did not propagated along a straight line as shown in Figs. 6(b and c). The propagation paths of many fine cracks were still blocked by the rigid aggregate and stones in concrete. This was because energy was required to propagate existing microcracks and create more new microcracks. But energy

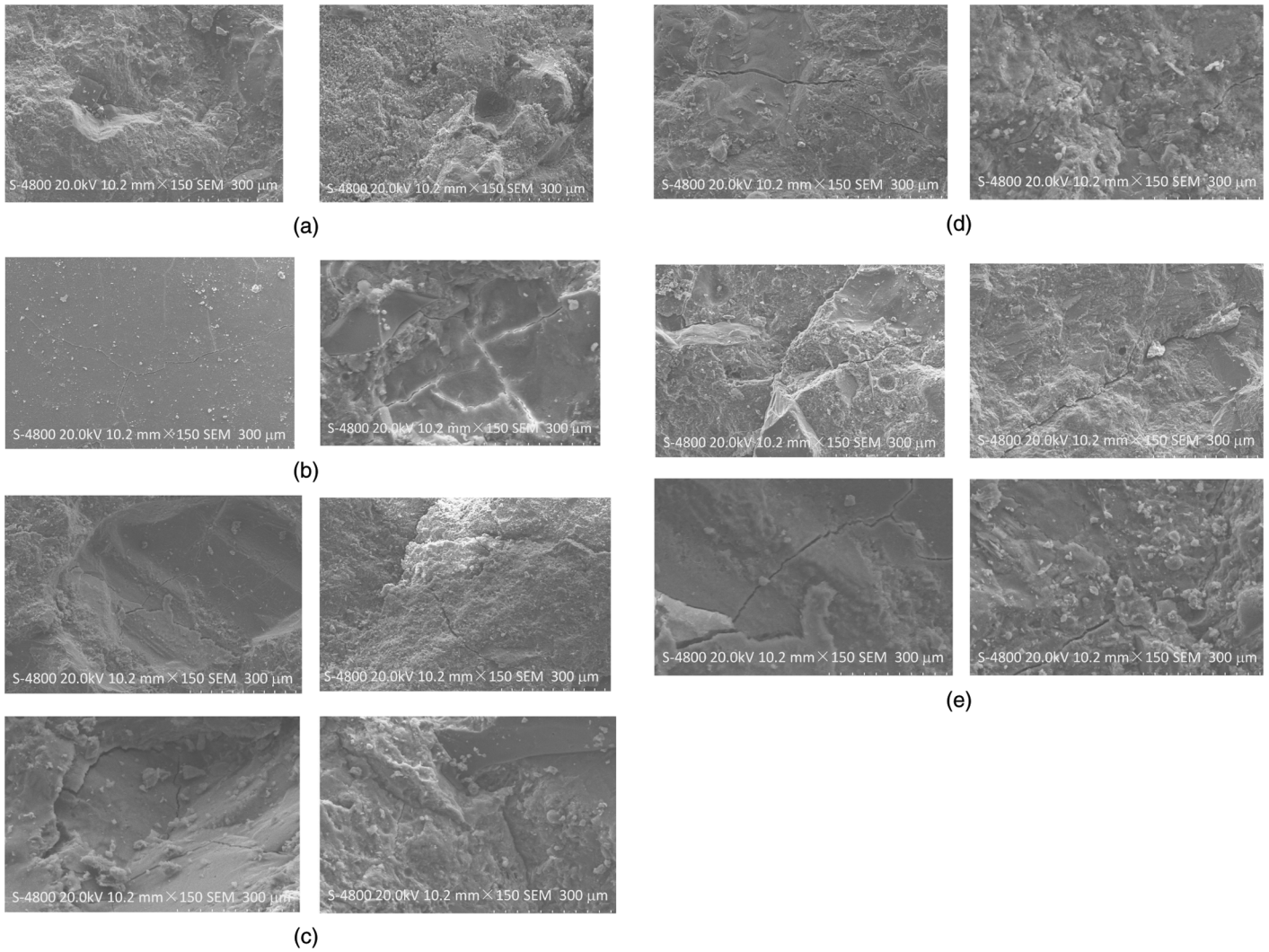

Fig. 6. Scanning electron micrographs for concrete under different initial static loading: (a) 0%; (b) 25%; (c) 50%; (d) 75%; (e) 90%

produced by the external loading was not enough to resist the defensive power produced by the microscopic structure. Therefore, compared with concrete specimens without any initial damage, the dynamic tensile strength of concrete remained unchanged.

As the applied static loading exceeded 75% of the peak static strength, as shown in Figs. 6(d and e), small cracks extended and connected to each other rapidly. The width of microcracks grew wider, and their depth also grew. The aggregate interfaces and the transition zone also appeared with many small cracks that rapidly propagated along the cement paste matrix and connected to each other without being hindered by the coarse aggregate. The common interaction of large and fine cracks destroyed the microstructure of the specimen, which was no longer a hard body and gradually lost resistance. If external loads were provided, the concrete specimens would finally collapse Therefore, the dynamic tensile strength decreased.

In conclusion, the microstructural changes of initial static loading in concrete agreed with the changes seen of macrodynamic tensile strength.

Conclusions

Static bending tests and the SHPB dynamic bending tests of concrete were carried out in this paper and the influence of different initial static loading history on the dynamic tensile properties of concrete were explored. The initial static loadings were divided into five grades, namely, 0, 25, 50, 75, and 90% of static tensile strength, respectively. A large number of mesostructure images of specimens were obtained by the means of SEM and used to analyze the influence of microcracks' propagation on the dynamic performance of concrete. In addition, the Weibull distribution model was introduced to analyze the test results. The following conclusions were obtained:

1. The dynamic tensile strength increased significantly with the increase of strain rates. When the initial static loading level did not exceed 50%, dynamic strength remained basically unchanged, and when the initial static loading level was more than 75%, concrete dynamic strength decrease gradually;
2. Due to drying and self shrinkage interaction effects, some fine cracks were already present at the aggregate–paste interfaces prior to any damage. When the initial static loading level did not exceed 50%, the propagation path of the small cracks was blocked by the hard coarse aggregate in concrete. The energy produced by the external load was not enough to destroy the concrete's microstructure, so the dynamic tensile strength remained unchanged. When the initial static loading exceeded 75% of the fracture stress, the microcracks extended and connected to each other rapidly. Interaction of large and small cracks led to the destruction of the microstructure, the specimens gradually lost the ability to resist, and the concrete's dynamic tensile strength decreased. To sum up, the microstructural changes under initial static loading were in good agreement with the changes observed in dynamic tensile strength.

Acknowledgments

This research is based upon work supported by the National Natural Science Foundation of China (Grant No. 51509078), Natural Science Foundation of Jiangsu Province (Grant No. BK20150820), and the Fundamental Research Funds for the Central Universities (2016B06014) granted to the first author Dr. Xudong Chen. The authors also appreciate the anonymous reviewers and editors for their valuable suggestions and comments.

References

ASTM. (1979). "Standard test method for flexural strength of concrete (using simple beam with center-point loading)." *ASTM-C293-02*, West Conshohocken, PA.

Bisschop, J., and Van Mier, J. G. M. (2002). "How to study drying shrinkage microcracking in cement-based materials using optical and scanning electron microscopy?" *Cem. Concr. Res.*, 32(2), 279–287.

Chen, X., Wu, S., and Zhou, J. (2013). "Experimental and modeling study of dynamic mechanical properties of cement paste, mortar and concrete." *Constr. Build. Mater.*, 47(10), 419–430.

Chen, X., Wu, S., and Zhou, J. (2014a). "Quantification of dynamic tensile behavior of cement-based materials." *Constr. Build. Mater.*, 51(1), 15–23.

Chen, X., Wu, S., and Zhou, J. (2014b). "Strength values of cementitious materials in bending and tension test methods." *J. Mater. Civ. Eng.*, 10.1061/(ASCE)MT.1943-5533.0000846, 484–490.

Cornelissen, H. A. W., and Reinhardt, H. W. (1984). "Uniaxial tensile fatigue failure of concrete under constant-amplitude and programme loading." *Mag. Concr. Res.*, 36(129), 216–226.

Cunliffe, C., Mehta, Y. A., Cleary, D., Ali, A., and Redles, T. (2015). "Impact of dynamic loading on backcalculated stiffness of rigid airfield pavements." *Int. J. Pavement Eng.*, 17(6), 489–502.

Delvare, F., Hanus, J. L., and Bailly, P. (2010). "A non-equilibrium approach to processing Hopkinson Bar bending test data: Application to quasi-brittle materials." *Int. J. Impact Eng.*, 37(12), 1170–1179.

Derucher, K. N. (1978). "Application of the scanning electron microscope to fracture studies of concrete." *Build. Environ.*, 13(2), 135–141.

GB/T (Standardization Administration of China). (2014). "Technical code for application of fly ash concrete." *GB/T 50146*, National Standard of the People's Republic of China, Beijing (in Chinese).

Gettu, R., Aguado, A., and Oliveira, M. O. F. (1996). "Damage in high-strength concrete due to monotonic and cyclic compression-a study based on splitting tensile strength." *ACI Mater. J.*, 93(6), 519–523.

Gupta, Y. M., and Seaman, L. (1978). "Local response of reinforced concrete to missile impacts." *Nucl. Eng. Des.*, 45(2), 507–514.

Konin, A., Francois, R., and Arliguie, G. (1998). "Analysis of progressive damage to reinforced ordinary and high performance concrete in relation to loading." *Mater. Struct.*, 31(1), 27–35.

Lin, G., Lu, J., Wang, Z., and Xiao, S. (2002). "Study on the reduction of tensile strength of concrete due to triaxial compressive loading history." *Mag. Concr. Res.*, 54(2), 113–124.

Lin, G., Yan, D., and Yuan, Y. (2007). "Response of concrete to dynamic elevated-amplitude cyclic tension." *ACI Mater. J.*, 104(6), 561–566.

Lu, J., Lin, G., Wang, Z., and Xiao, S. (2004). "Reduction of compressive strength of concrete due to triaxial compressive loading history." *Mag. Concr. Res.*, 56(3), 139–149.

Singh, M., Lakshmi, V., and Srivastava, L. P. (2015). "Effect of pre-loading with tensile stress on laboratory UCS of a synthetic rock." *Rock Mech. Rock Eng.*, 48(1), 53–60.

Soroushian, P., and Elzafraney, M. (2004). "Damage effects on concrete performance and microstructure." *Cem. Concr. Compos.*, 26(7), 853–859.

Tinic, C., and Brühwiler, E. (1985). "Effect of compressive loads on the tensile strength of concrete at high strain rates." *Int. J. Cem. Compos. Lightweight Concrete*, 7(2), 103–108.

Uchikawa, H., Hanehara, S., and Hirao, H. (1997). "Influence of microstructural change under stress on the strength-related properties of hardened cement mortar and paste." *Adv. Cem. Based Mater.*, 6(3), 87–98.

Wang, X. S., Wu, B. S., and Wang, Q. Y. (2005). "Online SEM investigation of microcrack characteristics of concretes at various temperatures." *Cem. Concr. Res.*, 35(7), 1385–1390.

Wu, Y., Yun, Y., Wei, Y., and Zhou, Y. (2014). "Effect of predamage on the stress-strain relationship of confined concrete under monotonic loading." *J. Struct. Eng.*, 10.1061/(ASCE)ST.1943-541X.0001015, 04014093.

Xiao, S., Li, H., and Monteiro, P. J. (2011). "Influence of strain rates and loading histories on the compressive damage behaviour of concrete." *Mag. Concr. Res.*, 63(12), 915–926.

Xiao, S., Li, H., and Monteiro, P. J. M. (2010). "Influence of strain rates and load histories on the tensile damage behaviour of concrete." *Mag. Concr. Res.*, 62(12), 887–894.

Yan, D., and Lin, G. (2008). "Influence of initial static stress on the dynamic properties of concrete." *Cem. Concr. Compos.*, 30(4), 327–333.

Zhao, H., and Gary, G. (1996). "On the use of SHPB techniques to determine the dynamic behavior of materials in the range of small strains." *Int. J. Solids Struct.*, 33(23), 3363–3375.